

Nonthermal emission of energetic ions from a metal surface irradiated by extremely low-fluence femtosecond laser pulses

Yasuhiro Miyasaka, Masaki Hashida, Yoshinobu Ikuta, Kazuto Otani, Shigeki Tokita, and Shuji Sakabe

Advanced Research Center for Beam Science, Institute for Chemical Research, Kyoto University, Gokasho, Uji, Kyoto 611-0011, Japan and Department of Physics, Graduate School of Science, Kyoto University, Kitashirakawa, Sakyo, Kyoto 606-8502, Japan

(Received 27 January 2012; revised manuscript received 5 June 2012; published 13 August 2012)

Energetic ions are emitted from a metal (copper) surface irradiated with femtosecond laser pulses even at extremely low laser fluences. The nonthermal interaction of the pulses with the metal surface is investigated by energy spectroscopy of ions emitted from the surface. Singly charged ions with energies of 180 eV are produced at low fluences of 80 mJ/cm², and the ion energy spectrum does not follow a shifted Maxwell-Boltzmann distribution. As the mechanism of ion acceleration, Coulomb explosion of nanoparticles on the target surface is proposed. This mechanism is supported by the fairly good agreement between calculated and experimental ion energy spectra and by the relationships of ion energy and ion emission amount with self-organized nanostructures formed on the irradiated surface.

DOI: [10.1103/PhysRevB.86.075431](https://doi.org/10.1103/PhysRevB.86.075431)

PACS number(s): 79.20.Eb, 79.70.+q, 79.77.+g

Femtosecond laser pulses interact with metal targets to bring about characteristic phenomena, for example, the formation of grating structures with subwavelength interspaces,^{1–5} the creation of amorphous metals,^{6,7} and extremely low ablation rates (less than one atomic layer on average).^{8,9} Accordingly, femtosecond lasers offer considerable promise for new applications.^{10–14} To utilize these phenomena, the exploration of the interaction physics is vital as is the development of laser technology.¹⁵ The ablation rate of copper under femtosecond laser irradiation has been measured precisely, and three sharp reductions in the rate occur at three laser fluences (here, called the low, middle, and high thresholds).⁸ These thresholds are explained by multiphoton absorption assisted by optical field distortion.¹⁶ Most of the above-mentioned phenomena occur at fluences between the middle and the high thresholds. In this fluence range, the ablation of metals has been investigated by many groups,^{17–27} and the process is well understood to be subject to laser absorption, thermal energy transport, and subsequent evaporation. However, little research has been conducted on the phenomena that occur between the low and the middle thresholds (here, called the low-fluence range).

We have found a new phenomenon of energetic ion emission in this low-fluence range. In this paper, ions emitted from a copper surface are studied by energy spectroscopy. The energy spectra of ions are investigated considering surface-state changes with respect to the number of laser pulses. A new mechanism of ion acceleration, namely, Coulomb explosion of nanoparticles (CENs), is proposed to explain the energy spectra of ions. This mechanism is supported by the relationships of surface-state (self-organized nanostructures) with ion energy and ion emission amounts.

Laser pulses (wavelength: 800 nm; pulse duration: 170 fs; repetition rate: 10 Hz) from a chirped pulse amplification T⁶-laser system²⁸ are used for the present surface interaction studies. The transverse mode of the pulse is Gaussian. The *p*-polarized laser is focused with a lens (*f* = 30 cm) at an incident angle of 70° to the target normal. The laser spot on the metal surface is elliptical (minor axis: 140 μm; major axis: 400 μm) at the 1/*e* maximum intensity. The laser fluence

is 80–100 mJ/cm², obtained by changing laser energy at a fixed spot size. The energy distributions of emitted ions are measured by a time-of-flight (TOF) method. The emitted ions fly in a 1.45-m TOF tube evacuated at $\sim 1 \times 10^{-7}$ Pa and are detected by a microchannel plate (MCP) in the current mode placed perpendicular to the target surface.²⁹ No voltage is applied to the TOF flight tube. Metal meshes connected to a bias voltage source are placed in front of the MCP and are used as energy filters to identify the ion species. High fluence is required for multiply charged copper ion generation,¹⁶ and Cu_{*m*}^{*n*+} (*n* = 1, *m* > 2) is not detected in TOF mass measurement. Therefore, we can identify the ion species from the cutoff time in TOF spectra corresponding to the voltage applied to the energy filters. The same position on the target is irradiated with thousands of pulses, and the ion energy distribution is obtained from ion signals averaged every 100 laser pulses. Before the first pulse, the target is moved to expose a fresh surface. The target is copper metal (99.99% pure, 20 mm × 20 mm, and 1-mm thick). To investigate the influence of the target surface morphology on ion emission, two targets with different morphologies [fresh and preirradiated (PI)] are used. Initially, both targets are mechanically polished to less than 1-nm roughness (arithmetic mean) and are washed in acetone with an ultrasonic cleaner. The PI target is irradiated before testing with 600 laser pulses at 140 mJ/cm², whereas, the fresh target is used as is after cleaning.

Figure 1 shows field-emission scanning electron microscopy (FE-SEM) images of fresh and PI target surfaces before and after irradiation at 80 mJ/cm². On the fresh target, nanoparticles formed by mechanical polishing are observed [Fig. 1(a)]. The size distribution of nanoparticles is lognormal, the median radius is 7.7 nm, and the standard deviation of the logarithmic radius is 0.41. On the PI target surface before testing [Fig. 1(b)], nanostructures are distributed on periodic grating structures with interspaces of ~ 3 μm.³⁰ Upon further irradiation, the density of nanostructures becomes smaller at the 1000th pulse [Fig. 1(c)], and nanostructures are not observed at the 20000th pulse [Fig. 1(d)]. Figure 2 shows typical TOF spectra obtained upon irradiation of fresh and PI targets with 100 pulses at 80 mJ/cm². Emitted ions are

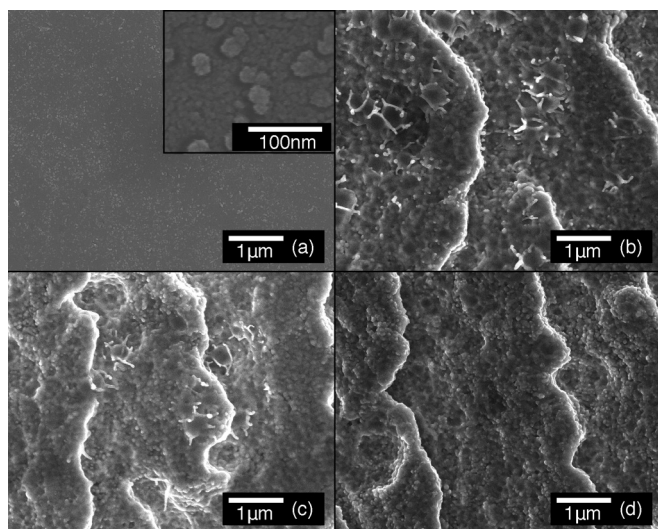


FIG. 1. FE-SEM images of (a) a fresh target surface and of (b) a PI target surface before testing, (c) at 1000 pulses, and (d) at 20 000 pulses at a laser fluence of 80 mJ/cm².

too few for a TOF spectrum to be acquired from a single pulse. The ion spectra averaged from the 1st to the 100th pulse [Figs. 2(a) and 2(b)] have a double-peak structure. The earlier and later peaks in the TOF spectra correspond to protons and singly charged copper ions, respectively. The ratio of H⁺ to Cu⁺ is less than 3% for the fresh target [Fig. 2(a)] and

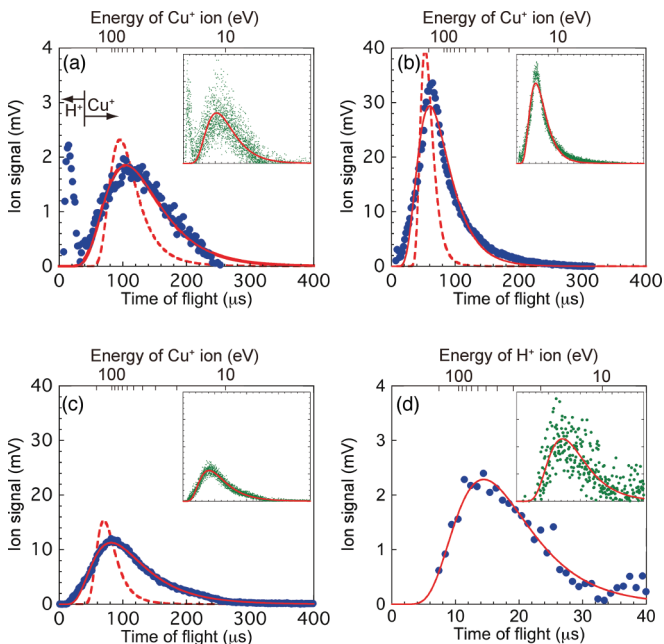


FIG. 2. (Color) TOF spectra averaged from the 1st to the 100th pulse (fluence: 80 mJ/cm²) for (a) a fresh target and (b) a PI target. (c) A TOF spectrum averaged from the 1001st to the 1100th pulse for a PI target (fluence: 80 mJ/cm²). (d) Expanded between 0 and 40 μs of (a). In the main plots, dots indicate data averaged every 2 μs. In the insets, dots indicate raw data. Dashed lines and solid lines indicate calculated SMB distribution and CEN distribution Eq. (3) of (a)–(c) a copper ion and (d) a proton, respectively. The physical parameters in the calculations are set to fit the experimental data.

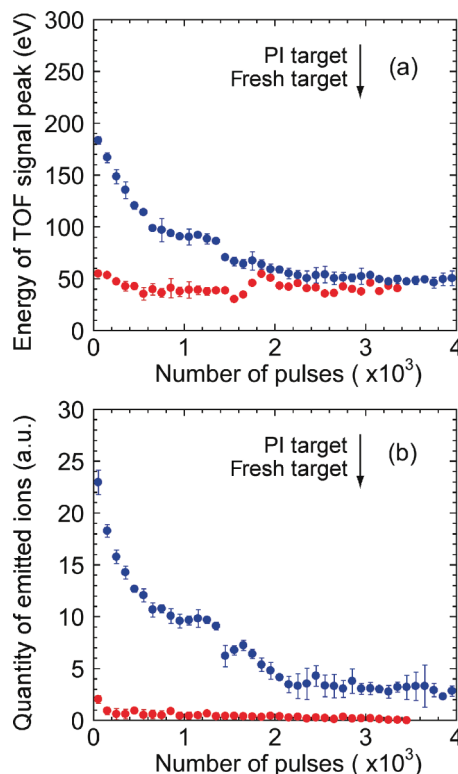


FIG. 3. (Color online) The dependence of (a) energy and (b) copper ion emission amounts on the number of laser pulses at 80 mJ/cm². The ion energy corresponds to the peak of the TOF signal. Upper and lower symbols are for the PI target and fresh target, respectively.

0.1% for the PI target [Fig. 2(b)]. However, the protons are not observed upon further irradiation (i.e., proton emission becomes negligible within the first 100 pulses of irradiation). This indicates that the protons are derived from molecules containing hydrogen, such as water, adsorbed on the target surface.^{31,32} The Cu⁺ ion peak corresponds to 50 eV for the fresh target [Fig. 2(a)] and to 180 and 90 eV for the PI target [Figs. 2(b) and 2(c)]. Both the ion energy and the ion emission amounts from the PI target are greater than those from the fresh target. This enhancement in ion emission might be related to the surface nanostructures seen in Fig. 1. The enhancement effect becomes weaker as more pulses are irradiated. Figure 3 shows the ion energy and ion emission amounts as functions of the number of laser pulses. To count the total emitted ions, the TOF spectrum is integrated over a time of flight from 0 to 400 μs. The contribution of H⁺ is small enough to ignore when estimating the total number of Cu⁺ ions from the PI target. As the number of pulses increases, the peak energy and ion emission amounts for the PI target tend to asymptotically approach those for the fresh target. PI targets, irradiated at different laser fluences (90 and 100 mJ/cm²), are also investigated. Figure 4 shows the ion emission properties of these fluences. The ion emission properties from Fig. 3 are also plotted. A greater number of pulses makes the PI target surface smoother, although the periodic structures remain as shown in Fig. 1. From the PI target irradiated with 20 000 pulses, only a few ions are emitted, and the TOF spectrum can no longer be obtained. This result suggests that ions are emitted from the

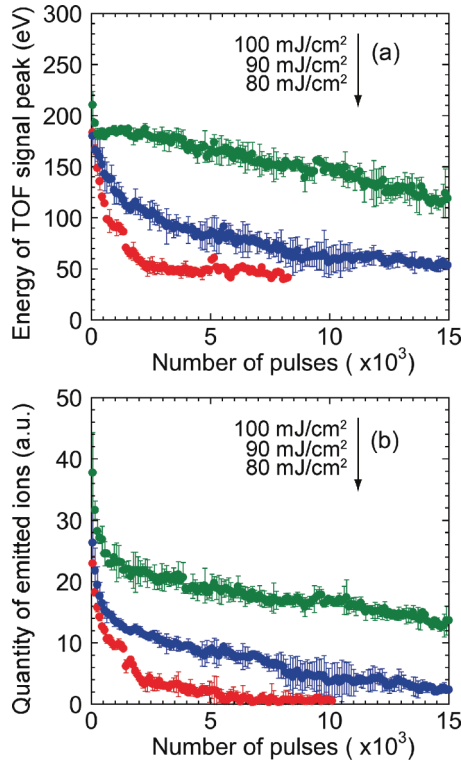


FIG. 4. (Color online) The dependence of (a) energy and (b) the amount of copper ions on number of laser pulses for the PI target. The upper, middle, and lower symbols are for laser fluences of 100, 90, and 80 mJ/cm², respectively.

nanostructures rather than from the periodic grating structures and that Cu⁺ ion emission is closely related to the nanoscale features of the surface morphology. For ions produced by high-fluence femtosecond and nanosecond laser ablation, the energy spectra usually follow a shifted Maxwell-Boltzmann (SMB) distribution.^{22,33,34} The dashed lines in Fig. 2 indicate the least-squares fits of the SMB distribution expressed as $f_{\text{SMB}}(t) = A/t^4 \exp[-m(L/t - v)^2/(2k_B T)]$, where A is the distribution normalization constant, t is the time of flight, m is the ion mass, L is the length of the TOF tube, v is the velocity of the center of mass of the emitted ions, k_B is the Boltzmann constant, and T is the temperature. In this experiment, $L = 1.45$ m and $m = 1.05 \times 10^{-25}$ kg for copper. The center-of-mass velocity is calculated from the TOF spectra, and the temperature is obtained by least-squares fitting of the SMB distribution to the experimental data: $v = 11.7, 23.4,$ and 16.5 km/s, and $T = 1.0 \times 10^5, 2.0 \times 10^5,$ and 1.6×10^5 K for Figs. 2(a)–2(c), respectively. The calculated TOF spectra, assuming an SMB distribution, are much different from the experimental results, and moreover, such high temperatures are unrealistic given the extremely low laser fluence used in the present experiment. As a mechanism of nonthermal ion emission, optical rectification has been proposed by Vella *et al.*³⁵ During laser irradiation, a rectified field is induced on the target surface, and the field accelerates ions. The intensity of the field depends on the target surface morphology. Following the method reported in Ref. 35, we calculate the energy of ions for our experimental conditions. To do so, we first calculate an effective local-field factor L_{eff} according to Ref. 36. We use the threshold dc field

for ion emission $F_{\text{th}} = 31$ V/nm,³⁷ the nonlinear susceptibility $|\chi_{S,zzz}^{(2)}| = 7.2 \times 10^{-16}$ m²/V,³⁸ and the rectified field length $l_p = 2.5$ Å.³⁵ The results show that the energy of emitted copper ions predicted by optical rectification is more than 10 keV, which is 2 orders higher than the energy observed in our experiment. Therefore, we conclude that optical rectification is not applicable under our experimental conditions. Another mechanism that must be considered is one where the field induced by emitted electrons during laser irradiation accelerates ions.³⁹ Under this mechanism, ion energy would be proportional to laser spot diameter. However we do not observe such a phenomenon under our experimental conditions. From the experimental results for ion properties with respect to surface morphology, we propose the following mechanism of ion emission to explain the TOF spectra: Initially, a small amount of nanoparticles exist [Fig. 1(a)], and considerably more nanostructures are formed by self-organization on the target surface under laser pulse irradiation; the nanostructures are Coulomb exploded by subsequent laser pulses, and nanostructures become smaller resulting in no more ion emissions. The TOF spectra are quantitatively reproduced under the following three assumptions. (a) When nanostructures are generated on the target surface by laser pulse irradiation, the nanostructures are treated as nanoparticles, and their radii have a lognormal distribution,⁴⁰

$$f_{\text{LN}}(r) = \frac{B}{\sqrt{2\pi}rw} \exp\left[-\frac{\{\ln(r/r_c)\}^2}{2w^2}\right], \quad (1)$$

where w is the standard deviation of the logarithmic radius and r_c is the median radius. Note, however, that the size distribution reported by Amoruso *et al.*⁴⁰ is obtained from the clusters produced on an opposing plate; hence, we assume that clusters come down in the target surface as well as the opposing plate. (b) The nanoparticle is ionized by a laser pulse, and ions are emitted from the nanoparticle surface by Coulomb explosion.⁴¹ In this CEN process (here, we assume that particles are spherical), the energy of the emitted ions is governed by the Coulomb potential $U = Ne^2/(4\pi\epsilon_0 r)$, where r is the nanoparticle radius, N is a number of ionized nanoparticles generated, e is the elementary charge, and ϵ_0 is the vacuum permittivity. (c) The number of ionized atoms in nanoparticles is proportional to the volume occupied by nanoparticles⁴² $N = 4\pi r^3 ni/3$, where n is the number density and i is the ionization rate. Under these assumptions, the time of flight is given by

$$t = L\sqrt{\frac{3\epsilon_0 m}{2nie^2}} \frac{1}{r}. \quad (2)$$

The number of emitted ions is dependent on the size distribution of nanoparticles and is proportional to the surface area of the nanoparticles. The distribution of emitted ions is described by $4\pi r^2 f_{\text{LN}}(r)$, and r is expressed in terms of t from Eq. (2),

$$f_{\text{CEN}}(t) = \frac{C}{t^3} \exp\left[-\frac{1}{2w^2} \left\{ \ln\left(\frac{L\sqrt{3\epsilon_0 m/(2ne^2)}}{tr_c\sqrt{i}}\right) \right\}^2\right], \quad (3)$$

where C is a distribution normalization constant, $L = 1.45$ m, $\epsilon_0 = 8.85 \times 10^{-12}$ F/m, $e = 1.60 \times 10^{-19}$ C, $m = 1.05 \times 10^{-25}$ kg, and $n = 8.85 \times 10^{28}$ m $^{-3}$ for copper. The solid lines in Fig. 2 are the least-squares fits of Eq. (3) to the energy spectra. From the values of $r_c = 7.7$ nm and $w = 0.41$ for the fresh target, an ionization rate of $i = 0.072\%$ is obtained by the least-squares fit of Eq. (3) to the data of Fig. 2(a). Using the ionization rate of $i = 0.072\%$, the least-squares fits of the CEN distribution to the experimental data are obtained for $r_c = 13$ and 7.8 nm and $w = 0.42$ and 0.50 for Figs. 2(b) and 2(c), respectively. The TOF spectra calculated by the CEN are in fairly good agreement with the experimental data. r_c in Fig. 2(b) is larger than that in Fig. 2(a), which is explained by the production of larger nanoparticles on the PI target than on the fresh target. The reduction in r_c from Figs. 2(b) to 2(c) corresponds to the nanoparticles becoming smaller due to Coulomb explosion at their surfaces under further pulse irradiation. Although r_c in Fig. 2(a) is equal to that in Fig. 2(c), the peak energies in these figures are different. The results shown in Fig. 2(c) suggest that the PI target surface has nanoparticles produced both by 140-mJ/cm^2 preirradiation pulses and by the subsequent 80-mJ/cm^2 -pulse irradiation. This is also shown by the difference in w . Figure 2(d) shows a TOF spectrum between 0 and $40\ \mu\text{s}$, expanded from Fig. 2(a). Protons are the main component. The solid line shows the CEN spectrum of protons calculated by using Eq. (3) with the parameters used in the copper ion calculations, except for the mass of the ion. The TOF spectrum is reproduced

fairly well by the CEN process. Therefore, the protons on the copper nanoparticles Coulomb explode under the same potential as copper ions do. This proton spectrum also supports the proposed CEN interpretation of ion emission.

In conclusion, even at extremely low laser fluences, femtosecond laser pulses generated energetic ion emission from a metal surface. The energy did not follow a Maxwell-Boltzmann distribution. Both the ion energy and the ion emission amounts were closely related to the surface morphology of the target. On the surface irradiated by femtosecond laser pulses at low fluences, nanostructures, such as nanoparticles, formed by self-organization. A mechanism of energetic ion emission was proposed. The Coulomb explosion of nanoparticles, formed by self-organization on the surface under femtosecond pulse irradiation, provides a reasonably good explanation for the experimental results obtained by TOF spectroscopy of the ions emitted from the fresh and PI targets.

We thank K. Hirao, T. Kanaya, and K. Nishida for their assistance with FE-SEM and SEM. This research was financially supported by a Grant-in-Aid for the Global COE Program “The Next Generation of Physics, Spun from Universality and Emergence” from the Ministry of Education, Culture, Sports, Science and Technology (MEXT) of Japan and was supported, in part, by the Amada Foundation for Metal Work Technology and a Grant-in Aid for Scientific Research Grant No. (C)(22560720) from MEXT, Japan.

-
- ¹K. Okamuro, M. Hashida, Y. Miyasaka, Y. Ikuta, S. Tokita, and S. Sakabe, *Phys. Rev. B* **82**, 165417 (2010).
- ²A. Y. Vorobyev, V. S. Makin, and C. Guo, *J. Appl. Phys.* **101**, 034903 (2007).
- ³Q. Z. Zhao, S. Malzer, and L. J. Wang, *Opt. Lett.* **32**, 1932 (2007).
- ⁴J. Wang and C. Guo, *J. Appl. Phys.* **100**, 023511 (2006).
- ⁵A. Y. Vorobyev and C. Guo, *Phys. Rev. B* **72**, 195422 (2005).
- ⁶M. Hashida, Y. Miyasaka, Y. Ikuta, S. Tokita, and S. Sakabe, *Phys. Rev. B* **83**, 235413 (2011).
- ⁷Y. Hirayama, P. A. Atanasov, M. Obara, N. N. Nedialokv, and S. E. Imamova, *Jpn. J. Appl. Phys.* **45**, 792 (2006).
- ⁸M. Hashida, A. F. Semerok, O. Gobert, G. Petite, Y. Izawa, and J. F. Wagner, *Appl. Surf. Sci.* **197–198**, 862 (2002).
- ⁹S. E. Kirkwood, M. T. Taschuk, Y. Y. Tsui, and R. Fedosejevs, *J. Phys.: Conf. Ser.* **59**, 591 (2007).
- ¹⁰A. Blatter, M. Maillat, S. M. Pimenov, G. A. Shafeev, and A. V. Simakin, *Tribol. Lett.* **4**, 237 (1998).
- ¹¹X. Wang, C. A. Ohlin, Q. Lu, and J. Hu, *Biomaterials* **29**, 2049 (2008).
- ¹²M. Barberoglou, V. Zorba, A. Pagoza, C. Fotakis, and E. Stratakis, *Langmuir* **26**, 13007 (2010).
- ¹³S. Matsumoto, A. Yane, S. Nakashima, M. Hashida, M. Fujita, Y. Goto, and S. Takahashi, *J. Am. Chem. Soc.* **129**, 3840 (2007).
- ¹⁴S. Kim, J. Jin, Y. J. Kim, I. Y. Park, Y. Kim, and S. W. Kim, *Nature (London)* **453**, 757 (2008).
- ¹⁵P. Russbuedt, T. Mans, J. Weitenberg, H. D. Hoffmann, and R. Poprawe, *Opt. Lett.* **35**, 4169 (2010).
- ¹⁶M. Hashida, S. Namba, K. Okamuro, S. Tokita, and S. Sakabe, *Phys. Rev. B* **81**, 115442 (2010).
- ¹⁷S. Sakabe, M. Hashida, S. Tokita, S. Namba, and K. Okamuro, *Phys. Rev. B* **79**, 033409 (2009).
- ¹⁸S. Amoruso, X. Wang, C. Altucci, C. de Lisio, M. Armenante, R. Bruzzese, and R. Velotta, *Appl. Phys. Lett.* **77**, 3728 (2000).
- ¹⁹Y. Okano, H. Kishimura, A. Yazaki, F. Saito, Y. Hironaka, K. G. Nakamura, K. Kondo, and Y. Oguri, *J. Surf. Sci. Soc. Jpn.* **22**, 438 (2001).
- ²⁰T. Donnelly, J. G. Lunney, S. Amoruso, R. Bruzzese, X. Wang, and X. Ni, *J. Appl. Phys.* **108**, 043309 (2010).
- ²¹G. O. Williams, G. M. O’Conner, P. T. Mannion, and T. J. Glynn, *Appl. Surf. Sci.* **254**, 5921 (2008).
- ²²M. Ye and C. P. Grigoropoulos, *J. Appl. Phys.* **89**, 5183 (2001).
- ²³N. Zhang, X. Zhu, J. Yang, X. Wang, and M. Wang, *Phys. Rev. Lett.* **99**, 167602 (2007).
- ²⁴R. Stoian, A. Rosenfeld, D. Ashkenasi, I. V. Hertel, N. M. Bulgakova, and E. E. B. Campbell, *Phys. Rev. Lett.* **88**, 097603 (2002).
- ²⁵V. Schmidt, W. Husinsky, and G. Betz, *Phys. Rev. Lett.* **85**, 3516 (2000).
- ²⁶M. E. Povarnitsyn, T. E. Itina, K. V. Khishchenko, and P. R. Levashov, *Phys. Rev. Lett.* **103**, 195002 (2009).
- ²⁷H. Dachraoui and W. Husinsky, *Appl. Phys. Lett.* **89**, 104102 (2006).
- ²⁸S. Tokita, M. Hashida, S. Masuno, S. Namba, and S. Sakabe, *Opt. Express* **16**, 14875 (2008).

- ²⁹J. Kou, V. Zhakhovskii, S. Sakabe, K. Nishihara, S. Shimizu, S. Kawato, M. Hashida, K. Shimizu, S. Bulanov, Y. Izawa, Y. Kato, and N. Nakashima, *J. Chem. Phys.* **112**, 5012 (2000).
- ³⁰T. Y. Yong and C. Guo, *J. Appl. Phys.* **108**, 073523 (2010).
- ³¹A. Henig, D. Kiefer, M. Geissler, S. G. Rykovanov, R. Ramis, R. Hörlein, J. Osterhoff, Z. Major, L. Veisz, S. Karsch, F. Krausz, D. Habs, and J. Schreiber, *Phys. Rev. Lett.* **102**, 095002 (2009).
- ³²D. Needly, P. Foster, A. Robinson, F. Lindau, O. Lundh, A. Prsson, C.-G. Wahlström, and P. McKenna, *Appl. Phys. Lett.* **89**, 021502 (2006).
- ³³P. Écija, M. N. Sánchez Rayo, R. Martínez, B. Sierra, C. Redondo, F. J. Basterretxea, and F. Castaño, *Phys. Rev. A* **77**, 032904 (2008).
- ³⁴L. Torrisi, S. Gammino, L. Andò, and L. Laska, *J. Appl. Phys.* **91**, 4685 (2002).
- ³⁵A. Vella, B. Deconihout, L. Marrucci, and E. Santamato, *Phys. Rev. Lett.* **99**, 046103 (2007).
- ³⁶G. T. Boyd, T. Rasing, J. R. R. Leite, and Y. R. Shen, *Phys. Rev. B* **30**, 519 (1984).
- ³⁷D. G. Brandon, *Philos. Mag.* **14**, 803 (1966).
- ³⁸D. Krause, C. W. Teplin, and C. T. Rogers, *J. Appl. Phys.* **96**, 3626 (2004).
- ³⁹N. M. Bulgakova, A. V. Zhukov, W. Marine, A. Y. Vorobvey, and C. Guo, *Proc. SPIE* **7005**, 70050C (2008).
- ⁴⁰S. Amoruso, G. Ausanio, R. Bruzzese, L. Gagnaniello, L. Lanotte, M. Vitiello, and X. Wang, *Appl. Surf. Sci.* **252**, 4863 (2006).
- ⁴¹S. Sakabe, M. Hashida, S. Tokita, S. Namba, and K. Okamoto, *Phys. Rev. B* **79**, 033409 (2009).
- ⁴²U. Saalman, *Laser Phys.* **19**, 202 (2009).